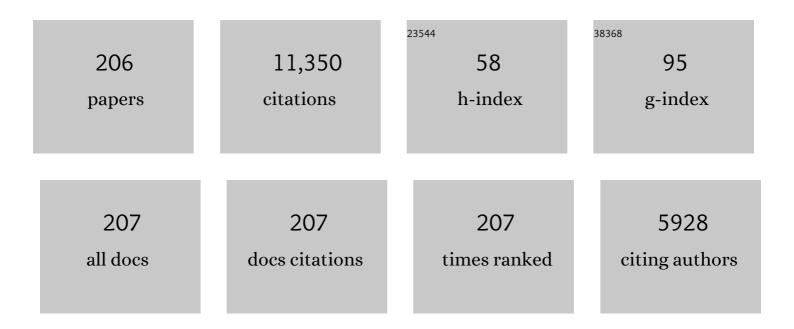
Mingying Peng

List of Publications by Year in descending order

Source: https://exaly.com/author-pdf/2419977/publications.pdf Version: 2024-02-01



#	Article	IF	CITATIONS
1	The reduction of Eu3+ to Eu2+ in BaMgSiO4â^¶Eu prepared in air and the luminescence of BaMgSiO4â^¶Eu2+ phosphor. Journal of Materials Chemistry, 2003, 13, 1202-1205.	6.7	352
2	Site Occupancy Preference, Enhancement Mechanism, and Thermal Resistance of Mn ⁴⁺ Red Luminescence in Sr ₄ Al ₁₄ O ₂₅ : Mn ⁴⁺ for Warm WLEDs. Chemistry of Materials, 2015, 27, 2938-2945.	3.2	309
3	Multi-functional bismuth-doped bioglasses: combining bioactivity and photothermal response for bone tumor treatment and tissue repair. Light: Science and Applications, 2018, 7, 1.	7.7	301
4	Band-Gap Modulation in Single Bi ³⁺ -Doped Yttrium–Scandium–Niobium Vanadates for Color Tuning over the Whole Visible Spectrum. Chemistry of Materials, 2016, 28, 2692-2703.	3.2	246
5	Highly Efficient and Thermally Stable K ₃ AlF ₆ :Mn ⁴⁺ as a Red Phosphor for Ultra-High-Performance Warm White Light-Emitting Diodes. ACS Applied Materials & Interfaces, 2017, 9, 8805-8812.	4.0	245
6	Controlling the Energy Transfer via Multi Luminescent Centers to Achieve White Light/Tunable Emissions in a Single-Phased X2-Type Y ₂ SiO ₅ :Eu ³⁺ ,Bi ³⁺ Phosphor For Ultraviolet Converted LEDs. Inorganic Chemistry, 2015, 54, 1462-1473.	1.9	241
7	Bismuth- and aluminum-codoped germanium oxide glasses for super-broadband optical amplification. Optics Letters, 2004, 29, 1998.	1.7	240
8	Superbroadband 1310 nm emission from bismuth and tantalum codoped germanium oxide glasses. Optics Letters, 2005, 30, 2433.	1.7	214
9	Study on the reduction of Eu3+→Eu2+ in Sr4Al14O25: Eu prepared in air atmosphere. Chemical Physics Letters, 2003, 371, 1-6.	1.2	213
10	Tunable Luminescent Properties and Concentration-Dependent, Site-Preferable Distribution of Eu ²⁺ Ions in Silicate Glass for White LEDs Applications. ACS Applied Materials & Interfaces, 2015, 7, 10044-10054.	4.0	197
11	400 mW ultrashort cavity low-noise single-frequency Yb^3+-doped phosphate fiber laser. Optics Letters, 2011, 36, 3708.	1.7	185
12	Discussion on the origin of NIR emission from Bi-doped materials. Journal of Non-Crystalline Solids, 2011, 357, 2241-2245.	1.5	173
13	Reduction from Eu3+ to Eu2+ in BaAl2O4:Eu phosphor prepared in an oxidizing atmosphere and luminescent properties of BaAl2O4:Eu. Journal of Luminescence, 2007, 127, 735-740.	1.5	172
14	Red Photoluminescence from Bi ³⁺ and the Influence of the Oxygen-Vacancy Perturbation in ScVO ₄ : A Combined Experimental and Theoretical Study. Journal of Physical Chemistry C, 2014, 118, 7515-7522.	1.5	164
15	Broadly tuning Bi ³⁺ emission via crystal field modulation in solid solution compounds (Y,Lu,Sc)VO ₄ :Bi for ultraviolet converted white LEDs. Journal of Materials Chemistry C, 2014, 2, 6068-6076.	2.7	164
16	Orderlyâ€Layered Tetravalent Manganeseâ€Doped Strontium Aluminate <scp><scp>Sr</scp></scp> ₄ <scp><scp>Al</scp></scp> ₁₄ <scp>An Efficient Red Phosphor for Warm White Light Emitting Diodes. Journal of the American Ceramic Society, 2013, 96, 2870-2876.</scp>	> ₂₅	: <scp: 154</scp:
17	Origin of broad NIR photoluminescence in bismuthate glass and Bi-doped glasses at room temperature. Journal of Physics Condensed Matter, 2009, 21, 285106.	0.7	153
	Abnormal Antiâ€Quenching and Controllable Multiâ€Transitions of Bi ³⁺ Luminescence by		

Abnormal Antia€Quenching and Controllable Multia€(ransitions of Bi³⁺ Luminescence by18Temperature in a Yellowâ€Emitting LuVO₄:Bi³⁺ Phosphor for UVâ€Converted1.7151White LEDs. Chemistry - A European Journal, 2014, 20, 11522-11530.

#	Article	IF	CITATIONS
19	Toward Bi ³⁺ Red Luminescence with No Visible Reabsorption through Manageable Energy Interaction and Crystal Defect Modulation in Single Bi ³⁺ -Doped ZnWO ₄ Crystal. Chemistry of Materials, 2017, 29, 8412-8424.	3.2	148
20	Redefinition of Crystal Structure and Bi ³⁺ Yellow Luminescence with Strong Near-Ultraviolet Excitation in La ₃ BWO ₉ :Bi ³⁺ Phosphor for White Light-Emitting Diodes. ACS Applied Materials & Interfaces, 2018, 10, 13660-13668.	4.0	144
21	Tunable dual-mode photoluminescence from nanocrystalline Eu-doped Li2ZnSiO4 glass ceramic phosphors. Journal of Materials Chemistry, 2011, 21, 3156.	6.7	128
22	Actively Targeted Deep Tissue Imaging and Photothermalâ€Chemo Therapy of Breast Cancer by Antibodyâ€Functionalized Drug‣oaded Xâ€Rayâ€Responsive Bismuth Sulfide@Mesoporous Silica Core–Shell Nanoparticles. Advanced Functional Materials, 2018, 28, 1704623.	7.8	120
23	Recoverable and Unrecoverable Bi ³⁺ -Related Photoemissions Induced by Thermal Expansion and Contraction in LuVO ₄ :Bi ³⁺ and ScVO ₄ :Bi ³⁺ Compounds. Chemistry of Materials, 2016, 28, 7807-7815.	3.2	114
24	Ultrabroad NIR luminescence and energy transfer in Bi and Er/Bi co-doped germanate glasses. Optics Express, 2011, 19, 20799.	1.7	106
25	Photoluminescence of Sr_2P_2O_7:Bi^2+ as a red phosphor for additive light generation. Optics Letters, 2010, 35, 2544.	1.7	104
26	Broadband NIR photoluminescence from Bi-doped Ba_2P_2O_7 crystals: Insights into the nature of NIR-emitting Bismuth centers. Optics Express, 2010, 18, 12852.	1.7	103
27	Investigations on bismuth and aluminum co-doped germanium oxide glasses for ultra-broadband optical amplification. Journal of Non-Crystalline Solids, 2005, 351, 2388-2393.	1.5	102
28	Visible to Nearâ€Infrared Persistent Luminescence and Mechanoluminescence from Pr ³⁺ â€Doped LiGa ₅ O ₈ for Energy Storage and Bioimaging. Advanced Optical Materials, 2019, 7, 1901107.	3.6	100
29	Broadband infrared luminescence from Li2O-Al2O3-ZnO-SiO2 glasses doped with Bi2O3. Optics Express, 2005, 13, 6892.	1.7	98
30	Luminescence from Bi^2+-activated alkali earth borophosphates for white LEDs. Optics Express, 2009, 17, 21169.	1.7	97
31	Intense red photoluminescence from Mn^2+-doped (Na^+; Zn^2+) sulfophosphate glasses and glass ceramics as LED converters. Optics Express, 2010, 18, 2549.	1.7	92
32	A new study on the energy transfer in the color-tunable phosphor CaWO ₄ :Bi. Dalton Transactions, 2014, 43, 277-284.	1.6	90
33	Near-infrared persistent phosphors: Synthesis, design, and applications. Chemical Engineering Journal, 2020, 399, 125688.	6.6	88
34	High Efficiency Mn ⁴⁺ Doped Sr ₂ MgAl ₂₂ O ₃₆ Red Emitting Phosphor for White LED. ECS Journal of Solid State Science and Technology, 2012, 1, R123-R126.	0.9	87
35	Bismuth-doped zinc aluminosilicate glasses and glass-ceramics with ultra-broadband infrared luminescence. Optical Materials, 2007, 29, 556-561.	1.7	86
36	Tailored Nearâ€Infrared Photoemission in Fluoride Perovskites through Activator Aggregation and Superâ€Exchange between Divalent Manganese Ions. Advanced Science, 2015, 2, 1500089.	5.6	86

#	Article	IF	CITATIONS
37	Temperature dependent red luminescence from a distorted Mn^4+ site in CaAl_4O_7:Mn^4+. Optics Express, 2013, 21, 18943.	1.7	85
38	Enhancing Osteosarcoma Killing and CT Imaging Using Ultrahigh Drug Loading and NIRâ€Responsive Bismuth Sulfide@Mesoporous Silica Nanoparticles. Advanced Healthcare Materials, 2018, 7, e1800602.	3.9	85
39	Selfâ€Recoverable Mechanically Induced Instant Luminescence from Cr ³⁺ â€Doped LiGa ₅ O ₈ . Advanced Functional Materials, 2021, 31, 2010685.	7.8	84
40	Superbroad near-to-mid-infrared luminescence from Bi_5 ^3+ in Bi_5(AlCl_4)_3. Optics Express, 2012, 20, 2562.	1.7	83
41	Emission color tuning through manipulating the energy transfer from VO ₄ ^{3â^'} to Eu ³⁺ in single-phased LuVO ₄ :Eu ³⁺ phosphors. Journal of Materials Chemistry C, 2017, 5, 390-398.	2.7	83
42	All-solid bandgap guiding in tellurite-filled silica photonic crystal fibers. Optics Letters, 2009, 34, 1946.	1.7	80
43	Heavily Eu ₂ O ₃ -doped yttria-aluminoborate glasses for red photoconversion with a high quantum yield: luminescence quenching and statistics of cluster formation. Journal of Materials Chemistry C, 2014, 2, 8678-8682.	2.7	80
44	Bismuth-doped oxide glasses as potential solar spectral converters and concentrators. Journal of Materials Chemistry, 2009, 19, 627-630.	6.7	79
45	The electronic and optical properties of a narrow-band red-emitting nanophosphor K ₂ NaGaF ₆ :Mn ⁴⁺ for warm white light-emitting diodes. Journal of Materials Chemistry C, 2018, 6, 3016-3025.	2.7	78
46	Low noise single-frequency single-polarization ytterbium-doped phosphate fiber laser at 1083Ânm. Optics Letters, 2013, 38, 501.	1.7	76
47	Broadband tunable near-infrared emission of Bi-doped composite germanosilicate glasses. Journal of Materials Chemistry, 2012, 22, 3154.	6.7	74
48	Broadly Tunable Emission from CaMoO ₄ :Bi Phosphor Based on Locally Modifying the Microenvironment Around Bi ³⁺ Ions. European Journal of Inorganic Chemistry, 2014, 2014, 1373-1380.	1.0	73
49	Hierarchical nickel oxide nanosheet@nanowire arrays on nickel foam: an efficient 3D electrode for methanol electro-oxidation. Catalysis Science and Technology, 2016, 6, 1157-1161.	2.1	73
50	Bi^2+-doped strontium borates for white-light-emitting diodes. Optics Letters, 2009, 34, 2885.	1.7	71
51	CaZnOS:Nd ³⁺ Emits Tissue-Penetrating near-Infrared Light upon Force Loading. ACS Applied Materials & Interfaces, 2018, 10, 14509-14516.	4.0	71
52	Generation of Emission Centers for Broadband NIR Luminescence in Bismuthate Glass by Femtosecond Laser Irradiation. Journal of the American Ceramic Society, 2009, 92, 542-544.	1.9	67
53	A new study on bismuth doped oxide glasses. Optics Express, 2012, 20, 15692.	1.7	67
54	Tuning the Eu luminescence in glass materials synthesized in air by adjusting glass compositions. Materials Letters, 2007, 61, 3608-3611.	1.3	65

#	Article	IF	CITATIONS
55	Bismuth-activated luminescent materials for broadband optical amplifier in WDM system. Journal of Non-Crystalline Solids, 2008, 354, 1221-1225.	1.5	65
56	Novel bismuth activated blue-emitting phosphor Ba ₂ Y ₅ B ₅ O ₁₇ :Bi ³⁺ with strong NUV excitation for WLEDs. Journal of Materials Chemistry C, 2019, 7, 11227-11233.	2.7	63
57	Preparation and optical properties of red, green and blue afterglow electrospun nanofibers. Journal of Materials Chemistry, 2011, 21, 2194-2203.	6.7	61
58	Broadband NIR luminescence from a new bismuth doped Ba_2B_5O_9Cl crystal: evidence for the Bi^0 model. Optics Express, 2012, 20, 22569.	1.7	60
59	Significantly conquering moisture-induced luminescence quenching of red line-emitting phosphor Rb ₂ SnF ₆ :Mn ⁴⁺ through H ₂ C ₂ O ₄ triggered particle surface reduction for blue converted warm white light-emitting diodes. Journal of Materials Chemistry C. 2019. 7. 247-255.	2.7	59
60	An investigation of the optical properties of Tb3+-doped phosphate glasses for green fiber laser. Optical Materials, 2012, 34, 1202-1207.	1.7	58
61	Efficient electrochemical water splitting catalyzed by electrodeposited NiFe nanosheets film. International Journal of Hydrogen Energy, 2016, 41, 8785-8792.	3.8	58
62	Ultraviolet-A Persistent Luminescence of a Bi ³⁺ -Activated LiScGeO ₄ Material. Inorganic Chemistry, 2020, 59, 12920-12927.	1.9	56
63	Orangeâ€ŧoâ€Red Emission from Bi ²⁺ and Alkaline Earth Codoped Strontium Borate Phosphors for White Light Emitting Diodes. Journal of the American Ceramic Society, 2010, 93, 1437-1442.	1.9	54
64	Epitaxial growth <i>via</i> anti-solvent-induced deposition towards a highly efficient and stable Mn ⁴⁺ doped fluoride red phosphor for application in warm WLEDs. Journal of Materials Chemistry C, 2019, 7, 6077-6084.	2.7	54
65	Processing-dependence and the nature of the blue-shift of Bi ³⁺ -related photoemission in ScVO ₄ at elevated temperatures. Journal of Materials Chemistry C, 2014, 2, 9850-9857.	2.7	53
66	Red to near infrared ultralong lasting luminescence from Mn ²⁺ -doped sodium gallium aluminum germanate glasses and (Al,Ga)-albite glass-ceramics. Journal of Materials Chemistry C, 2015, 3, 3406-3415.	2.7	53
67	Highly thermal-sensitive robust LaTiSbO6:Mn4+ with a single-band emission and its topological architecture for single/dual-mode optical thermometry. Chemical Engineering Journal, 2020, 384, 123272.	6.6	53
68	Bismuth activated high thermal stability blue-emitting phosphor Na ₂ Y ₂ B ₂ O ₇ :Bi used for near-UV white-light LEDs. Journal of Materials Chemistry C, 2020, 8, 16584-16592.	2.7	53
69	A promising blue-emitting phosphor CaYGaO ₄ :Bi ³⁺ for near-ultraviolet (NUV) pumped white LED application and the emission improvement by Li ⁺ ions. Journal of Materials Chemistry C, 2021, 9, 303-312.	2.7	53
70	GeO2: Bi,M (M=Ga,B) glasses with super-wide infrared luminescence. Chemical Physics Letters, 2005, 403, 410-414.	1.2	50
71	Unusual Concentration Induced Antithermal Quenching of the Bi2+ Emission from Sr2P2O7:Bi2+. Inorganic Chemistry, 2015, 54, 6028-6034.	1.9	50
72	Mechanoluminescence properties of Mn ²⁺ -doped BaZnOS phosphor. Journal of Materials Chemistry C, 2016, 4, 8166-8170.	2.7	50

#	Article	IF	CITATIONS
73	Site Occupancy Preference and Antithermal Quenching of the Bi ²⁺ Deep Red Emission in β-Ca ₂ P ₂ O ₇ :Bi ²⁺ . Inorganic Chemistry, 2017, 56, 6499-6506.	1.9	50
74	Photoluminescence of Bi^2+-doped BaSO_4 as a red phosphor for white LEDs. Optics Express, 2012, 20, A977.	1.7	49
75	Novel persistent and tribo-luminescence from bismuth ion pairs doped strontium gallate. Journal of Materials Chemistry C, 2018, 6, 10367-10375.	2.7	49
76	Tunable photoluminescence from YTaO ₄ :Bi ³⁺ for ultraviolet converted pc-WLED with high chromatic stability. Journal of Materials Chemistry C, 2020, 8, 6079-6085.	2.7	49
77	Site-specific reduction of Bi3+ to Bi2+ in bismuth-doped over-stoichiometric barium phosphates. Journal of Materials Chemistry C, 2013, 1, 5303.	2.7	48
78	Insights into luminescence quenching and detecting trap distribution in Ba ₂ Si ₅ N ₈ :Eu ²⁺ phosphor with comprehensive considerations of temperature-dependent luminescence behaviors. Journal of Materials Chemistry C, 2015, 3, 9572-9579.	2.7	48
79	Efficient Enhancement of Bismuth <scp>NIR</scp> Luminescence by Aluminum and Its Mechanism in Bismuthâ€Doped Germanate Laser Glass. Journal of the American Ceramic Society, 2016, 99, 2071-2076.	1.9	48
80	Near infrared mechanoluminescence from the Nd ³⁺ doped perovskite LiNbO ₃ :Nd ³⁺ for stress sensors. Journal of Materials Chemistry C, 2019, 7, 6301-6307.	2.7	48
81	Broadband NIR photoluminescence from Ni ²⁺ -doped nanocrystalline Ba–Al titanate glass ceramics. Journal of Materials Chemistry, 2012, 22, 2582-2588.	6.7	47
82	27Âî¼m emission in Er^3+:CaF_2 nanocrystals embedded oxyfluoride glass ceramics. Optics Letters, 2013, 38, 3071.	1.7	47
83	Broad-bandwidth near-shot-noise-limited intensity noise suppression of a single-frequency fiber laser. Optics Letters, 2016, 41, 1333.	1.7	47
84	Ultrabroadband near-Infrared Photoemission from Bismuth-Centers in Nitridated Oxide Glasses and Optical Fiber. ACS Photonics, 2018, 5, 4393-4401.	3.2	47
85	Recent Advances in Super Broad Infrared Luminescence Bismuth-Doped Crystals. IScience, 2020, 23, 101578.	1.9	46
86	Rechargeable and sunlight-activated Sr3Y2Ge3O12:Bi3+ UV–Visible-NIR persistent luminescence material for night-vision signage and optical information storage. Chemical Engineering Journal, 2021, 421, 127820.	6.6	46
87	Sr ₃ Y(BO ₃) ₃ :Bi ³⁺ phosphor with excellent thermal stability and color tunability for near-ultraviolet white-light LEDs. Journal of Materials Chemistry C, 2021, 9, 3672-3681.	2.7	46
88	Novel Bi-doped glasses for broadband optical amplification. Journal of Non-Crystalline Solids, 2008, 354, 1235-1239.	1.5	44
89	Spectral shifting and NIR down-conversion in Bi ³⁺ /Yb ³⁺ co-doped Zn ₂ GeO ₄ . Journal of Materials Chemistry C, 2014, 2, 8083-8088.	2.7	44
90	Mn ⁴⁺ -Doped Heterodialkaline Fluorogermanate Red Phosphor with High Quantum Yield and Spectral Luminous Efficacy for Warm-White-Light-Emitting Device Application. Inorganic Chemistry, 2018, 57, 14705-14714.	1.9	44

#	Article	IF	CITATIONS
91	Recent Advances in Mechanoluminescence of Doped Zinc Sulfides. Laser and Photonics Reviews, 2021, 15, 2100276.	4.4	44
92	Broadband near-infrared luminescence and tunable optical amplification around 1.55î¼m and 1.33î¼m of PbS quantum dots in glasses. Journal of Alloys and Compounds, 2011, 509, 9335-9339.	2.8	43
93	Synthesis and optical properties of chromium-doped spinel hollow nanofibers by single-nozzle electrospinning. RSC Advances, 2012, 2, 2773.	1.7	42
94	Creating and stabilizing Bi NIR-emitting centers in low Bi content materials by topo-chemical reduction and tailoring of the local glass structure. Journal of Materials Chemistry C, 2018, 6, 5384-5390.	2.7	42
95	Site Occupation of Eu ²⁺ in Ba _{2–<i>x</i>} Sr _{<i>x</i>} SiO ₄ (<i>x</i> = 0–1.9) and Origin of Improved Luminescence Thermal Stability in the Intermediate Composition. Inorganic Chemistry, 2018, 57, 7090-7096.	1.9	42
96	Anti-Stokes Fluorescent Probe with Incoherent Excitation. Scientific Reports, 2014, 4, 4059.	1.6	41
97	Wavelengthâ€Tunability and Multiband Emission from Singleâ€Site Mn ²⁺ Doped CaO Through Antiferromagnetic Coupling and Tailored Superexchange Reactions. Advanced Optical Materials, 2017, 5, 1700070.	3.6	40
98	Visible to near-infrared persistent luminescence from Tm ³⁺ -doped two-dimensional layered perovskite Sr ₂ SnO ₄ . Journal of Materials Chemistry C, 2019, 7, 8303-8309.	2.7	40
99	Cr ³⁺ -Free near-infrared persistent luminescence material LiGaO ₂ :Fe ³⁺ : optical properties, afterglow mechanism and potential bioimaging. Journal of Materials Chemistry C, 2020, 8, 14100-14108.	2.7	40
100	Thermal quenching of Mn4+ luminescence in SrAl12O19:Mn4+. Journal of Luminescence, 2019, 206, 84-90.	1.5	39
101	In situ growth of nickel selenide nanowire arrays on nickel foil for methanol electro-oxidation in alkaline media. RSC Advances, 2015, 5, 87051-87054.	1.7	38
102	Temperature dependence and quantum efficiency of ultrabroad NIR photoluminescence from Ni^2+centers in nanocrystalline Ba-Al titanate glass ceramics. Optics Letters, 2012, 37, 1166.	1.7	37
103	Synthesis and photoluminescence properties of a novel red phosphor SrLaGaO ₄ :Mn ⁴⁺ . Journal of the American Ceramic Society, 2019, 102, 1269-1276.	1.9	37
104	Force-induced 1540Ânm luminescence: Role of piezotronic effect in energy transfer process for mechanoluminescence. Nano Energy, 2020, 69, 104413.	8.2	37
105	Mixed Network Effect of Broadband Nearâ€Infrared Emission in <scp><scp>Bi</scp></scp> â€Doped <scp><scp>B</scp></scp> ₂ <scp><scp>O</scp></scp> ₃ â€ <scp><scp>GeO</scp><!--<br-->Glasses. Journal of the American Ceramic Society, 2012, 95, 3842-3846.</scp>	scp 1.9 sub	>2<\$ssub>
106	Luffa-Sponge-Like Glass–TiO ₂ Composite Fibers as Efficient Photocatalysts for Environmental Remediation. ACS Applied Materials & Interfaces, 2013, 5, 7527-7536.	4.0	36
107	Ultrabroad Photoemission from an Amorphous Solid by Topochemical Reduction. Advanced Optical Materials, 2018, 6, 1801059.	3.6	36
108	Near-infrared mechanoluminescence crystals: a review. IScience, 2021, 24, 101944.	1.9	36

#	Article	IF	CITATIONS
109	1120 nm kHz-linewidth single-polarization single-frequency Yb-doped phosphate fiber laser. Optics Express, 2016, 24, 29794.	1.7	35
110	Precise frequency shift of NIR luminescence from bismuth-doped Ta ₂ O ₅ –GeO ₂ glass via composition modulation. Journal of Materials Chemistry C, 2014, 2, 7830.	2.7	34
111	Homogeneity of bismuth-distribution in bismuth-doped alkali germanate laser glasses towards superbroad fiber amplifiers. Optics Express, 2015, 23, 12423.	1.7	34
112	Transparent Ni2+-doped ZnO–Al2O3–SiO2 system glass-ceramics with broadband infrared luminescence. Materials Research Bulletin, 2007, 42, 762-768.	2.7	33
113	Topoâ€Chemical Tailoring of Tellurium Quantum Dot Precipitation from Supercooled Polyphosphates for Broadband Optical Amplification. Advanced Optical Materials, 2016, 4, 1624-1634.	3.6	33
114	Noise-sidebands-free and ultra-low-RIN 15  μm single-frequency fiber laser towards coherent optical detection. Photonics Research, 2018, 6, 326.	3.4	33
115	Near infrared mechanoluminescence from Sr ₃ Sn ₂ O ₇ : Nd ³⁺ for in situ biomechanical sensor and dynamic pressure mapping. Journal of the American Ceramic Society, 2019, 102, 5899-5909.	1.9	33
116	Discovery of a novel rare-earth free narrow-band blue-emitting phosphor Y ₃ Al ₂ Ga ₃ O ₁₂ :Bi ³⁺ with strong NUV excitation for LCD LED backlights. Journal of Materials Chemistry C, 2020, 8, 13668-13675.	2.7	33
117	Origin of D-band emission in a novel Bi ³⁺ -doped phosphor La ₃ SnGa ₅ O ₁₄ :Bi ³⁺ . Journal of Materials Chemistry C, 2021, 9, 3455-3461.	2.7	33
118	Excitation wavelength-dependent near-infrared luminescence from Bi-doped silica glass. Journal of Alloys and Compounds, 2012, 531, 10-13.	2.8	32
119	Tuning Mn ⁴⁺ Red Photoluminescence in (K,Rb) ₂ Ge ₄ O ₉ :Mn ⁴⁺ Solid Solutions by Partial Alkali Substitution. Journal of the American Ceramic Society, 2016, 99, 3376-3381.	1.9	32
120	Deep red SrLaGa ₃ O ₇ :Mn ⁴⁺ for near ultraviolet excitation of white light LEDs. Journal of Materials Chemistry C, 2021, 9, 3969-3977.	2.7	32
121	kHz-order linewidth controllable 1550 nm single-frequency fiber laser for coherent optical communication. Optics Express, 2017, 25, 19752.	1.7	31
122	Synthesis, Structure, and Performance of Efficient Red Phosphor LiNaGe ₄ O ₉ :Mn ⁴⁺ and Its Application in Warm <scp>WLED</scp> s. Journal of the American Ceramic Society, 2016, 99, 2029-2034.	1.9	30
123	Broadband UV-to-green photoconversion in V-doped lithium zinc silicate glasses and glass ceramics. Optics Express, 2011, 19, A312.	1.7	29
124	Superbroad visible to NIR photoluminescence from Bi^+ evidenced in Ba_2B_5O_9Cl: Bi crystal. Optics Express, 2016, 24, 2830.	1.7	28
125	(INVITED) Recent advances in ultraviolet persistent phosphors. Optical Materials: X, 2019, 2, 100022.	0.3	28
126	Bismuth activated blue phosphor with high absorption efficiency for white LEDs. Journal of Alloys and Compounds, 2021, 885, 160960.	2.8	28

#	Article	IF	CITATIONS
127	Comparative investigation on the spectroscopic properties of Pr3+-doped boro-phosphate, boro-germo-silicate and tellurite glasses. Spectrochimica Acta - Part A: Molecular and Biomolecular Spectroscopy, 2012, 93, 223-227.	2.0	27
128	Formation, near-infrared luminescence and multi-wavelength optical amplification of PbS quantum dot-embedded silicate glasses. Journal of Non-Crystalline Solids, 2014, 383, 192-195.	1.5	27
129	Ultralong tumor retention of theranostic nanoparticles with short peptide-enabled active tumor homing. Materials Horizons, 2019, 6, 1845-1853.	6.4	27
130	Observation of Eu3+→Eu2+ in barium hexa-aluminates with β′ or β-alumina structures prepared in air. Optical Materials, 2004, 27, 591-595.	1.7	26
131	Morphology and phase control of fluorides nanocrystals activated by lanthanides with two-model luminescence properties. Nanoscale, 2012, 4, 4658.	2.8	26
132	915  nm all-fiber laser based on novel Nd-doped high alumina and yttria glass @ silica glass hybrid fiber for the pure blue fiber laser. Optics Letters, 2019, 44, 2153.	1.7	26
133	Defect Enrichment in Near Inverse Spinel Configuration to Enhance the Persistent Luminescence of Fe ³⁺ . Advanced Optical Materials, 2022, 10, 2101669.	3.6	26
134	Instant precipitation of KMgF ₃ :Ni ²⁺ nanocrystals with broad emission (1.3â€2.2Âl¼m) for potential combustion gas sensors. Journal of the American Ceramic Society, 2018, 101, 3890-3899.	1.9	25
135	Broadband NIR emission from multiple Bi centers in nitridated borogermanate glasses <i>via</i> tailoring local glass structure. Journal of Materials Chemistry C, 2019, 7, 2076-2084.	2.7	25
136	A Honeycombâ€Like Bismuth/Manganese Oxide Nanoparticle with Mutual Reinforcement of Internal and External Response for Tripleâ€Negative Breast Cancer Targeted Therapy. Advanced Healthcare Materials, 2021, 10, e2100518.	3.9	25
137	Superbroad near to mid infrared luminescence from closo-deltahedral Bi_5 ^3+ cluster in Bi_5(GaCl_4)_3. Optics Express, 2012, 20, 18505.	1.7	23
138	Compact all-fiber ring femtosecond laser with high fundamental repetition rate. Optics Express, 2012, 20, 24607.	1.7	23
139	Manipulating Bi NIR emission by adjusting optical basicity, boron and aluminum coordination in borate laser glasses. Journal of the American Ceramic Society, 2018, 101, 624-633.	1.9	23
140	Topological tailoring of structure and defects to enhance red to near-infrared afterglow from Mn ²⁺ -doped germanate photonic glasses. Journal of Materials Chemistry C, 2018, 6, 11525-11535.	2.7	23
141	Visualizing Dynamic Performance of Lipid Droplets in a Parkinson's Disease Model via a Smart Photostable Aggregation-Induced Emission Probe. IScience, 2019, 21, 261-272.	1.9	22
142	Selfâ€activated persistent luminescence from Ba ₂ Zr ₂ Si ₃ O ₁₂ for information storage. Journal of the American Ceramic Society, 2020, 103, 6922-6931.	1.9	22
143	Thermal degradation of ultrabroad bismuth NIR luminescence in bismuth-doped tantalum germanate laser glasses. Optics Letters, 2016, 41, 1340.	1.7	21
144	Multifunctional Cu ₃₉ S ₂₈ hollow nanopeanuts for in vivo targeted photothermal chemotherapy. Journal of Materials Chemistry B, 2017, 5, 6740-6751.	2.9	21

#	Article	IF	CITATIONS
145	Distribution and stabilization of bismuth NIR centers in Bi-doped aluminosilicate laser glasses by managing glass network structure. Journal of Materials Chemistry C, 2018, 6, 7814-7821.	2.7	21
146	Mechanism for broadening and enhancing Nd ³⁺ emission in zinc aluminophosphate laser glass by addition of Bi ₂ O ₃ . Journal of the American Ceramic Society, 2019, 102, 1694-1702.	1.9	20
147	New strategy to enhance the broadband nearâ€infrared emission of bismuthâ€doped laser glasses. Journal of the American Ceramic Society, 2018, 101, 2297-2304.	1.9	19
148	In situ instant generation of an ultrabroadband near-infrared emission center in bismuth-doped borosilicate glasses via a femtosecond laser. Photonics Research, 2019, 7, 300.	3.4	19
149	Composite film with anisotropically enhanced optical nonlinearity for a pulse-width tunable fiber laser. Journal of Materials Chemistry C, 2018, 6, 1126-1135.	2.7	18
150	Tunable luminescence from bismuthâ€doped phosphate laser glass by engineering photonic glass structure. Journal of the American Ceramic Society, 2018, 101, 1916-1922.	1.9	18
151	Tunable trap depth for persistent luminescence by cationic substitution in Pr 3+ :K 1â^ x Na x NbO 3 perovskites. Journal of the American Ceramic Society, 2018, 102, 2629.	1.9	18
152	Boosting the branching ratio at 900 nm in Nd ³⁺ doped germanophosphate glasses by crystal field strength and structural engineering for efficient blue fiber lasers. Journal of Materials Chemistry C, 2019, 7, 11824-11833.	2.7	18
153	Controllable fabrication and broadband near-infrared luminescence of various Ni2+-activated ZnAl2O4 nanostructures by a single-nozzle electrospinning technique. Physical Chemistry Chemical Physics, 2012, 14, 13594.	1.3	17
154	Tunable emission color and mixed valence state via the modified activator site in the AlN-doped Sr ₃ SiO ₅ :Eu phosphor. RSC Advances, 2016, 6, 33076-33082.	1.7	17
155	Visible and Near-Infrared Emission in Ba ₃ Sc ₄ O ₉ :Bi Phosphor: An Investigation on Bismuth Valence Modification. Inorganic Chemistry, 2021, 60, 13510-13516.	1.9	17
156	Prediction on Mn ⁴⁺ â€Doped Germanate Red Phosphor by Crystal Field Calculation on Basis of Exchange Charge Model: A Case Study on K ₂ Ge ₄ O ₉ :Mn ⁴⁺ . Journal of the American Ceramic Society, 2016, 99, 2388-2394.	1.9	16
157	Tailoring Cluster Configurations Enables Tunable Broad-Band Luminescence in Glass. Chemistry of Materials, 2020, 32, 8653-8661.	3.2	16
158	The role of oxygen defects in a bismuth doped ScVO ₄ matrix: tuning luminescence by hydrogen treatment. Journal of Materials Chemistry C, 2017, 5, 314-321.	2.7	15
159	Compact passively Q-switched single-frequency Er ³⁺ /Yb ³⁺ codoped phosphate fiber laser. Applied Physics Express, 2017, 10, 052502.	1.1	14
160	Dual-wavelength passively q-switched single-frequency fiber laser. Optics Express, 2016, 24, 16149.	1.7	13
161	Tailoring super-broad photoluminescence from Eu2+and dual-mode Eu2+/Eu3+-doped alkaline earth aluminoborate glasses through site-similarity and ligand acidity. Journal of Luminescence, 2016, 180, 234-240.	1.5	13
162	The origin of the heterogeneous distribution of bismuth in aluminosilicate laser glasses. Journal of the American Ceramic Society, 2018, 101, 2921-2929.	1.9	13

#	Article	IF	CITATIONS
163	Enhanced <scp>NIR</scp> photoemission from Biâ€doped aluminoborate glasses via topological tailoring of glass structure. Journal of the American Ceramic Society, 2019, 102, 1710-1719.	1.9	13
164	Unusual anti-thermal degradation of bismuth NIR luminescence in bismuth doped lithium tantalum silicate laser glasses. Optics Express, 2016, 24, 18649.	1.7	12
165	Feature issue introduction: persistent and photostimulable phosphors – an established research field with clear challenges ahead. Optical Materials Express, 2016, 6, 1414.	1.6	12
166	Novel compositions of Bi 2 O 3 -ZnO-TeO 2 glasses: Structure and hardness analysis. Journal of Non-Crystalline Solids, 2017, 464, 23-29.	1.5	12
167	Self-injection locked and semiconductor amplified ultrashort cavity single-frequency Yb^3+-doped phosphate fiber laser at 978 nm. Optics Express, 2017, 25, 1535.	1.7	12
168	Predictable tendency of Bi <scp>NIR</scp> emission in Biâ€doped magnesium aluminosilicate laser glasses. Journal of the American Ceramic Society, 2018, 101, 1159-1168.	1.9	12
169	Near quantum-noise limited and absolute frequency stabilized 1083  nm single-frequency fiber laser. Optics Letters, 2018, 43, 42.	1.7	12
170	Spectroscopic properties of Sm3+-doped phosphate glasses. Journal of Materials Research, 2012, 27, 2111-2115.	1.2	11
171	Frequency noise of distributed Bragg reflector single-frequency fiber laser. Optics Express, 2017, 25, 12601.	1.7	11
172	Temperature dependent energy transfer in Bi/Er codoped barium gallogermanate glasses for tunable and broadband NIR emission. Journal of Materials Chemistry C, 2019, 7, 10544-10550.	2.7	11
173	A New Red Aluminate Phosphor CaAl ₁₂ O ₁₉ Activated by Bi ₂ ⁺ for White LEDs. Science of Advanced Materials, 2017, 9, 485-489.	0.1	11
174	Ultra-broadband red to NIR photoemission from multiple bismuth centers in Sr ₂ B ₅ O ₉ Cl:Bi crystal. Optics Letters, 2019, 44, 4821.	1.7	11
175	Comment on "Enhanced room-temperature emission in Cr4+ ions containing alumino-silicate glasses― [Appl. Phys. Lett. 82, 4035 (2003)]. Applied Physics Letters, 2005, 87, 066103.	1.5	10
176	Unusual concentration induced antithermal quenching of the Eu 2+ emission at 490 nm in Sr 4 Al 14 O 25 :Eu 2+ for near ultraviolet excited white LEDs. Journal of the American Ceramic Society, 2020, 103, 5758-5768.	1.9	10
177	Fluorescence properties and laser demonstrations of Nd-doped high silica glasses prepared by sintering nanoporous glass. Journal of Non-Crystalline Solids, 2008, 354, 1226-1229.	1.5	9
178	Controllable Synthesis and Peculiar Optical Properties of Lanthanideâ€Doped Fluoride Nanocrystals. ChemPlusChem, 2014, 79, 601-609.	1.3	9
179	Crystallization kinetics and enhanced Bi NIR luminescence of transparent silicate glassâ€ceramics containing Sr ₂ YbF ₇ nanocrystals. Journal of the American Ceramic Society, 2017, 100, 574-582.	1.9	9
180	D2h-Symmetric Tetratellurium Clusters in Silicate Glass as a Broadband NIR Light Source for Spectroscopy Applications. ACS Applied Materials & Interfaces, 2020, 12, 51628-51636.	4.0	9

#	Article	IF	CITATIONS
181	Unusual thermal response of tellurium near-infrared luminescence in phosphate laser glass. Optics Letters, 2018, 43, 4823.	1.7	9
182	Microstructural modification of chalcogenide glasses by femtosecond laser. Journal of Non-Crystalline Solids, 2011, 357, 2392-2395.	1.5	8
183	Classâ€forming region and enhanced Bi NIR emission in sodium tantalum silicate laser glass. Journal of the American Ceramic Society, 2019, 102, 2522-2530.	1.9	8
184	Enhancement of ultrabroadband Bi NIR emission via fluorination for all wavelength amplification of optical communication. Journal of the American Ceramic Society, 2021, 104, 1309-1317.	1.9	8
185	Regulating the Bi NIR luminescence behaviours in fluorine and nitrogen co-doped germanate glasses. Materials Advances, 2021, 2, 4743-4751.	2.6	8
186	Improving luminescence behavior and glass stability of telluriumâ€doped germanate glasses by modifying network topology. Journal of the American Ceramic Society, 2022, 105, 929-937.	1.9	8
187	A femtosecond hybrid mode-locking fiber ring laser at 409 MHz. Laser Physics Letters, 2013, 10, 085104.	0.6	6
188	An introduction to the 2nd International Workshop on Persistent and Photostimulable Phosphors (IWPPP 2013). Optical Materials, 2014, 36, 1769-1770.	1.7	6
189	Long persistent luminescence in Mn^2+-activated sodium gallium germanate glass and glass ceramics induced by infrared femtosecond laser pulses. Optical Materials Express, 2016, 6, 2380.	1.6	6
190	Cancer Nanotheranostics: Actively Targeted Deep Tissue Imaging and Photothermalâ€Chemo Therapy of Breast Cancer by Antibodyâ€Functionalized Drug‣oaded Xâ€Rayâ€Responsive Bismuth Sulfide@Mesoporous Silica Core–Shell Nanoparticles (Adv. Funct. Mater. 5/2018). Advanced Functional Materials, 2018, 28, 1870034.	7.8	6
191	Ultra-compact all-fiber narrow-linewidth single-frequency blue laser at 489 nm. Journal of Optics (United Kingdom), 2018, 20, 025803.	1.0	6
192	Quantitative prediction of the structure and properties of Li ₂ O–Ta ₂ O ₅ –SiO ₂ glasses via phase diagram approach. Journal of the American Ceramic Society, 2019, 102, 185-194.	1.9	6
193	Suppressing the thermal degradation of bismuth near-infrared luminescence in optical amorphous materials via topologically polymerized network structures. Journal of Materials Chemistry C, 2019, 7, 5074-5083.	2.7	6
194	Abnormal NIR photoemission from bismuth doped germanophosphate photonic glasses. Journal of Materials Chemistry C, 2019, 7, 3218-3225.	2.7	6
195	Flexible and thermally stable SiO2–TiO2 composite micro fibers with hierarchical nano-heterostructure. RSC Advances, 2013, 3, 20132.	1.7	5
196	Palladium speciation in UVâ€ŧransparent glasses. Journal of the American Ceramic Society, 2020, 103, 4214-4223.	1.9	5
197	Modulating broadband near infrared emission from Bi doped borate laser glass by codoping nonactive rare earth ions. Journal of Non-Crystalline Solids, 2021, 553, 120477.	1.5	5
198	Topological control of negatively charged local environments for tuning bismuth NIR luminescence in glass materials. Journal of Alloys and Compounds, 2022, 898, 162884.	2.8	5

#	Article	IF	CITATIONS
199	Tunable broadband near-infrared luminescence in glass realized by defect-engineering. Optics Express, 2021, 29, 32149.	1.7	4
200	All fiber ring bound-soliton laser with a round trip time of 5.7 ns. Optics Communications, 2012, 285, 5449-5451.	1.0	3
201	Fabrication of Silica Nano/Micro-Fibers Doped with One-Dimensional Assembly of Silver Nanoparticles. Journal of Nanoscience and Nanotechnology, 2013, 13, 325-332.	0.9	3
202	Deep red radioluminescence from a divalent bismuth doped strontium pyrophosphate Sr ₂ P ₂ O ₇ :Bi ²⁺ . Proceedings of SPIE, 2015, , .	0.8	3
203	Photoemission from Biâ€doped calcium aluminate glasses similar to sunlight. Journal of the American Ceramic Society, 2019, 102, 2542-2550.	1.9	3
204	Low Temperature Spectroscopic Properties of Divalent Bismuth Doped Ba2P2O7 for White Light LEDs. Science of Advanced Materials, 2017, 9, 490-494.	0.1	3
205	Selective self-redox and crystal field modulation for enhanced and tuned broadband emission in chromium-doped aluminate glasses. Journal of Materials Chemistry C, 2019, 7, 5401-5409.	2.7	2
206	Bismuth-Doped Photonic Materials: Are They Promising Phosphors for WLEDs?. , 2017, , 421-457.		1